

# Are broad optical balmer lines from central accretion disk in PG 1613+658?

Zhang, Xue-Guang<sup>1,2</sup>

<sup>1</sup>*Purple Mountain Observatory, Chinese Academy of Sciences, 2 Beijing XiLu, NanJing, JiangSu, 210008, P. R. China*

<sup>2</sup>*Chinese Center for Antarctic Astronomy, NanJing, JiangSu, 210008, P. R. China*

## ABSTRACT

In this letter, we report positive correlations between broad line width and broad line flux for the broad balmer lines of the long-term observed AGN PG 1613+658. Rather than the expected negative correlations under the widely accepted virialization assumption for AGN BLRs, the positive correlations indicate much different BLR structures of PG 1613+658 from the commonly considered BLR structures which are dominated by the equilibrium between radiation pressure and gas pressure. Therefore, accretion disk origin is preferred for the observed broad single-peaked optical balmer lines of PG 1613+658, because of the mainly gravity dominated disk-like BLRs with radial structures having few effects from radiation pressure.

**Key words:** Galaxies:Active – Galaxies:nuclei – Galaxies:quasars:Emission lines – Galaxies: Individual: PG 1613+658

## 1 INTRODUCTION

Broad emission line regions (BLRs) of active galactic nuclei (AGNs) so far can not be resolved spatially, however, many efforts have been done to study geometric and dynamic structures of AGN BLRs by properties of spectroscopic and photometric variability (Blandford & McKee 1982, Peterson et al. 1993, Bentz et al. 2010, Pancoast et al. 2011, Grier et al. 2013, Kollatschny & Zetzl 2011, 2013, Pancoast et al. 2013, Baskin et al. 2014, Kollatschny et al. 2014). Moreover, under the commonly and widely accepted virialization assumption for AGN BLRs, properties of broad emission lines can be applied to conveniently estimate virial black hole masses of broad line AGNs (Peterson et al. 2004, Kelly & Bechtold 2007, Krause et al. 2011, Woo et al. 2013, Ho & Kim 2014):

$$M_{BH} \propto V_{broad}^2 \times R_{BLRs} \propto V_{broad}^2 \times \lambda L_{5100\text{\AA}}^{0.5} \quad (1)$$

where  $V_{broad}$  represents broad line width which can be treated as the substitute for rotating velocities of broad line emission clouds,  $R_{BLRs}$  means the distance between BLRs and central black hole (the BLRs size) which can be estimated by the empirical relation  $R_{BLRs} \propto \lambda L_{5100\text{\AA}}^{0.5}$  (Wang & Zhang 2003, Kaspi et al. 2005, Bentz et al. 2013). Moreover, with the considerations of the strong correlation between continuum luminosity and broad line luminosity (Greene & Ho 2005), the equation above can be re-written as

$$M_{BH} \propto V_{broad}^2 \times L_{broad}^{0.5} \quad (2)$$

From the equation above, we can expect one strong negative correlation between broad line width and broad line lumi-

osity,  $V_{broad}^2 \times L_{broad}^{0.5} = \text{constant}$ , for individual long-term observed AGN.

Several AGNs have been reported on the expected negative correlations between broad line width and broad line luminosity (or BLR size) (Peterson et al. 2004), however, in our previous papers on 3C390.3 (Zhang 2013a) and PG 0052+251 (Zhang 2013b), we have reported unexpected positive correlations between broad line width and broad line luminosity for the double-peaked broad  $H\alpha$  of 3C390.3 and for the intermediate broad component of optical balmer lines of PG 0052+521. Here, we report one another positive correlation between broad line width and broad line flux of broad balmer lines in PG 1613+658, and then give further discussions on the probable origin of broad balmer lines from central accretion disk. The letter is organized as follows. Section 2 gives our main results. Section 3 shows our discussions and conclusions.

## 2 MAIN RESULTS

PG 1613+658 (=PG1613) is one well known long-term observed AGN in the sample of Kaspi et al. (2000). There are 44 public optical spectra with both broad  $H\beta$  and broad  $H\alpha$ , which can be collected from the website <http://wise-obs.tau.ac.il/~shai/PG/>. The detailed descriptions about the observing techniques and reduction procedures for the public spectra can be found in Kaspi et al. (2000). The collected spectra observed from 21th, May, 1991 to 16th, Sep., 1998 have been binned into  $1\text{\AA}$  per pixel and

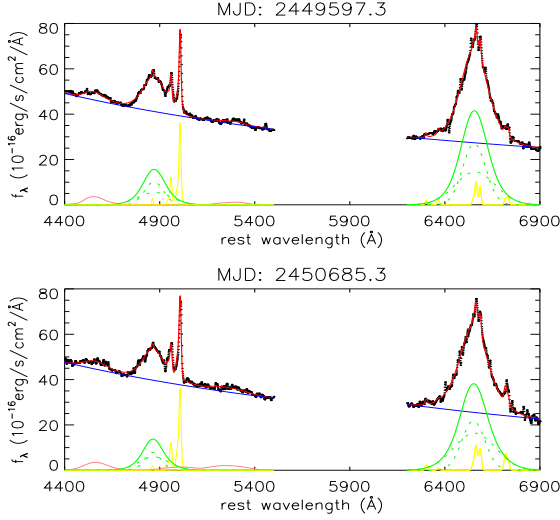


**Figure 1.** Two examples on the best fitted results for emission lines in the spectra observed on 1th, Sep. 1994 and observed on 24th, Aug. 1997. In each panel, solid line in black represents the observed spectrum, solid line in red are for the best fitted results, solid line in blue is for the power law AGN continuum, solid lines in green, yellow and pink near the bottom are for the broad line, for the narrow emission lines and for the optical Fe II respectively, dotted lines in green are the two determined broad gaussian components.

been padded from 3000Å to 9000Å. Then, line parameters of emissions of PG1613 are measured as follows

All the emission lines are fitted simultaneously within the rest wavelength ranges from 4400Å to 5500Å and from 6200Å to 6900Å. Here, for each broad balmer emission line, two broad gaussian functions rather than one broad gaussian function are applied, because of complicate broad line profile. For optical Fe II lines, the more recent optical Fe II template in Kovacevic et al. (2010) has been applied in our procedure. For narrow emission lines (narrow balmer lines, [O III]λ4959, 5007Å, [O I]λ6300, 6363Å, [N II]λ6548, 6583Å and [S II]λ6716, 6731Å doublets), they are described by narrow gaussian functions with similar line profiles, i.e., they have the same emission line redshift, the same line width. Furthermore, one broad gaussian function is applied for the much weak He II line, and two extended broad components are applied for the extended wings of [O III] doublet. And moreover, the [O III] and [N II] doublets have the fixed theoretical flux ratios expected by atomic physics: the flux ratios of [O III]λ5007Å to [O III]λ4959Å and [N II]λ6583Å to [N II]λ6548Å are fixed to 3 (Dimitrijevic et al. 2007). Then, two independent power law functions are applied for the AGN continuum under the Hβ and under the Hα. Finally, line parameters can be well determined through Levenberg-Marquardt least-squares minimization method. Figure 1 shows two examples on the best fitted results for the emission lines, including each determined broad line described by two broad gaussian components.

Then, after subtractions of the narrow emission lines, the continuum emission, the Fe II lines and the He II line, we will have the clear broad line profile (similar as the sum of the determined two broad gaussian components), and measure line parameters through the broad line profile. Here,

**Table 1.** Line Parameters

MJD	$\sigma(H\beta)$	flux(Hβ)	$\sigma(H\alpha)$	flux(Hα)	flux
48425	3359±109	21.0±0.6	3425±108	78.0±2.2	97.5±2.8
48426	3639±123	20.2±0.5	3699±124	74.9±1.9	92.8±2.4
48835	4024±143	21.7±0.6	3269±99	71.4±2.2	82.9±2.6
49095	2932±89	17.4±0.3	3308±101	71.6±1.4	88.9±1.7
49157	3969±140	19.4±0.4	3477±111	69.3±1.6	86.5±2.0
49220	3957±139	18.3±0.4	3412±107	71.3±1.9	84.2±2.2
49249	4280±157	23.3±0.8	3561±116	69.5±2.3	92.8±3.2
49282	3712±126	23.7±0.4	3348±104	80.3±1.4	106.±1.9
49426	3523±117	19.1±0.5	3654±121	77.0±2.1	98.5±2.7
49453	3902±136	21.3±0.5	3891±136	74.7±1.8	94.6±2.3
49487	3744±128	21.9±0.3	3565±116	73.9±1.2	97.5±1.6
49519	4752±185	23.6±0.5	4367±168	85.0±1.9	99.5±2.3
49541	4464±168	23.4±0.2	4273±161	82.5±1.0	99.0±1.2
49569	4256±156	22.5±0.3	4261±160	83.5±1.1	99.0±1.4
49597	4330±160	24.5±0.3	3878±135	79.3±1.2	99.1±1.5
49597	4368±162	23.1±0.3	4100±149	85.2±1.1	101.±1.4
49784	4792±188	24.6±0.5	4079±148	81.6±1.7	98.3±2.1
49813	4806±189	24.5±0.3	4099±149	80.7±1.1	99.2±1.4
49828	4413±165	24.1±0.2	4079±148	85.2±1.0	102.±1.2
49838	4592±176	23.7±0.3	4192±156	85.0±1.1	101.±1.3
49876	4276±157	23.5±0.3	4119±151	80.3±1.0	99.8±1.3
49897	4413±165	22.4±0.4	4329±165	81.3±1.7	97.3±2.1
49915	4040±144	22.1±0.2	3728±126	77.4±0.8	94.9±1.0
49919	4571±174	21.4±0.5	4167±154	78.5±1.8	95.6±2.2
49962	4200±153	20.6±0.3	4050±146	76.7±1.3	94.1±1.6
49984	4455±168	23.3±0.3	3947±139	76.7±1.1	94.8±1.4
49989	4205±153	22.7±0.1	3791±130	80.1±0.6	98.7±0.7
50191	4531±172	23.9±0.6	4151±153	84.5±2.3	102.±2.8
50198	4393±164	24.6±0.2	3964±141	86.8±0.8	103.±1.0
50241	3989±141	22.1±0.4	3925±138	78.2±1.5	99.2±1.9
50244	4089±147	22.9±0.3	3875±135	84.9±1.2	104.±1.4
50287	4129±149	22.9±0.2	3894±136	80.2±0.9	98.1±1.1
50310	3781±130	19.3±0.7	3890±136	74.6±3.0	93.2±3.7
50313	4771±187	25.0±0.4	3809±131	74.5±1.3	93.7±1.6
50332	4504±170	20.9±0.2	3979±142	77.4±0.8	94.7±1.0
50580	3900±136	19.8±0.9	3583±117	68.0±3.3	81.8±4.0
50643	4877±193	22.2±0.4	3957±140	71.6±1.4	88.3±1.7
50685	4115±148	20.3±0.4	4177±155	77.7±1.7	95.3±2.1
50918	3876±135	22.9±1.1	4546±181	93.3±4.7	103.±5.2
50967	3979±141	23.5±0.3	4338±166	86.8±1.1	103.±1.3
51001	4634±178	24.8±0.9	4303±163	84.1±3.2	100.±3.8
51027	4489±170	25.6±0.6	4182±155	82.7±2.1	100.±2.5
51051	4418±165	25.0±0.3	4213±157	84.5±1.1	101.±1.3
51073	4566±174	24.8±0.7	4497±177	87.1±2.7	104.±3.2

Notice: the first column is MJD-2400000, the second and the third columns are the line width (the second moment) in unit of km/s and the line flux in unit of  $10^{-15}$  erg/s/cm<sup>2</sup> of broad Hβ, the fourth and the fifth columns are the line width and the line flux of broad Hα, the sixth column shows the line flux Hα including contributions from narrow emission lines collected from Kaspi et al. (2000).

second moment rather than FWHM (full width at half maximum) is preferred as the line width of broad lines, because the second moment is well defined for arbitrary line profiles and has relatively lower uncertainty (Fromerth & Melia 2000, Peterson et al. 2004). second moment ( $\sigma$ ) and line flux ( $flux$ ) are calculated by

$$flux = \int P_{\lambda} d\lambda$$

$$\sigma^2 = \frac{\int \lambda^2 \times P_{\lambda} d\lambda}{flux} - \left( \frac{\int \lambda \times P_{\lambda} d\lambda}{flux} \right)^2 \quad (3)$$

where  $P_{\lambda}$  represents broad line profile. Then, within the rest wavelength range from 4400Å to 5600Å for broad Hβ and 6000Å to 7200Å for broad Hα, the line parameters can be well determined for broad lines of PG1613, which are listed in Table 1.

Moreover, corresponding uncertainties of line parameters are calculated as follows. Because only wavelength and flux information are included in the collected spectra of PG1613, it is hard to determine more accurate uncertainties

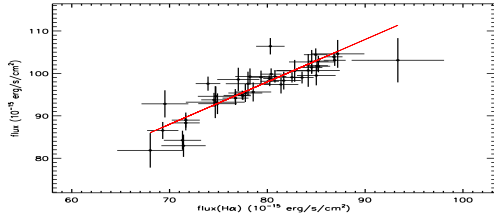


**Figure 2.** On the correlation between line flux of broad  $H\alpha$  ( $flux(H\alpha)$ ) measured from line profile of broad  $H\alpha$  and the reported line flux of  $H\alpha$  ( $flux$ ) in Kaspi et al. (2000) including contributions from narrow lines. The red line shows the correlation  $flux = flux(H\alpha) + 18$ .

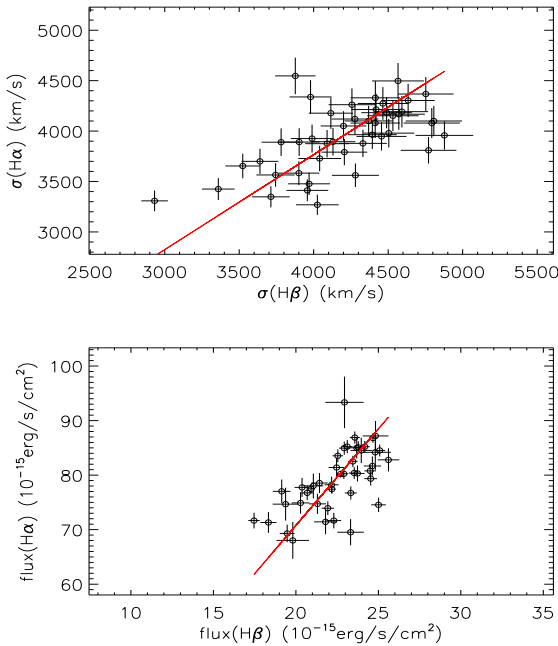


**Figure 3.** Top panel shows the line width correlation between broad  $H\alpha$  and broad  $H\beta$ . In the panel, solid line in red represents  $\sigma(H\alpha) = 0.95 \times \sigma(H\beta)$ . Bottom panel shows the line flux correlation between broad  $H\alpha$  and broad  $H\beta$ . In the panel, solid line in red shows  $flux(H\alpha) = 3.54 \times flux(H\beta)$ .

for broad line parameters. Therefore, the reported parameter uncertainties in Kaspi et al. (2000) have been applied. Based on the reported values and corresponding uncertainties of broad line flux (including contributions from narrow emission lines) in Kaspi et al. (2000)  $f_{k00} \pm ferr_{k00}$ , our measured broad line flux uncertainties are determined by  $f_{broad} * ferr_{k00} / f_{k00}$ , where  $f_{broad}$  represents our measured broad line flux after narrow lines being subtracted. Then, similar as estimations of uncertainties of broad line flux, the uncertainty in FWHM given in Kaspi et al. (2000) is applied to estimate the uncertainty for the second moment of broad line.

Then, based on measured line parameters of broad lines, we show correlations of broad line parameters for PG 1613. First and foremost, Figure 2 shows the correlation between the broad  $H\alpha$  line flux ( $flux(H\alpha)$ ) measured from line profile of broad  $H\alpha$  and the reported  $H\alpha$  line flux ( $flux$ ) in

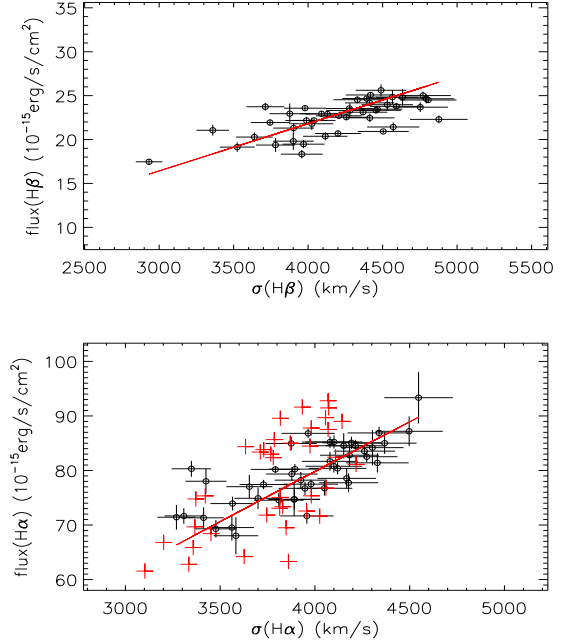


**Figure 4.** Correlations between line width and line flux for broad  $H\beta$  (top panel) and for broad  $H\alpha$  (bottom panel) respectively. In the panels, open circles are for line parameters from observed line profiles, solid lines in red are the corresponding best fitted results. In the bottom panel, symbol of plus in red is for the value from model expected broad  $H\alpha$  with accretion disk origin.

Kaspi et al. (2000) including contributions from narrow lines. The spearman rank correlation coefficient is 0.92 with  $P_{null} < 5 \times 10^{-7}$ . The strong linear correlation and the best fitted result  $flux = flux(H\alpha) + 18$  indicate our fitted results for the broad  $H\alpha$  have high confidence levels. Therefore, there are no further discussions on the spectral flux calibrations or on the effects of narrow lines on our following results. Besides, Figure 3 shows the line parameter correlations between broad  $H\alpha$  and broad  $H\beta$ . Top panel shows the line width correlation between broad  $H\alpha$  and broad  $H\beta$ . Bottom panel shows the line flux correlation between broad  $H\alpha$  and broad  $H\beta$ . The spearman rank correlation coefficients are 0.59 with  $P_{null} \sim 10^{-5}$  and 0.67 with  $P_{null} \sim 10^{-6}$  for the broad line width correlation and for the broad line flux correlation respectively. The strong correlations further support the high confidence levels for our measured broad line parameters to some extent. Last but not least, Figure 4 shows the correlation between broad line width and broad line flux for broad balmer lines. The spearman rank correlation coefficients are 0.67 with  $P_{null} \sim 10^{-6}$  and 0.76 with  $P_{null} \sim 10^{-9}$  for the correlations by parameters of broad  $H\beta$  and by parameters of broad  $H\alpha$  respectively. Then, with considerations of the uncertainties in both coordinates, the results can be well described as

$$\begin{aligned} \log(flux(H\beta)) &\propto (0.99 \pm 0.07) \times \log(\sigma(H\beta)) \\ \log(flux(H\alpha)) &\propto (0.92 \pm 0.08) \times \log(\sigma(H\alpha)) \end{aligned} \quad (4)$$

. It is clear that the results are not consistent with the expected result  $\sigma^2 \times flux^{0.5} \sim constant$  under the virialization assumption for AGN BLRs.

### 3 DISCUSSIONS AND CONCLUSIONS

It is interesting to discuss what BLR structures should lead to the unexpected positive correlations between broad line width and broad line flux shown in Figure 4. In our previous papers on 3C390.3 (Zhang 2013a) and on PG0052+251 (Zhang 2013b), broad lines coming from central accretion disks are considered for the positive correlations. Here, in the letter, some further discussions on the BLR structures should be given.

As commonly discussed BLRs, such as the more recent discussions in Baskin et al. (2014) (and references therein), the radiation pressure has an important role on radial structures of AGN BLRs. And moreover, the model in Baskin et al. (2014) makes definite predictions that are easily tested with just the flux and width measurements of the broad lines. We should test the model as follows. Through the equilibrium between radiation pressure and gas pressure, AGN BLR size sensitively depends on continuum luminosity (also on broad line luminosity, due to the strong correlation between continuum luminosity and broad line luminosity). Therefore, the flux weighted BLR size being increased with continuum being stronger leads to one strongly expected negative correlation between broad line width and broad line luminosity. In order to find unexpected strong positive correlations for broad lines, the other model on the BLR structures should be considered, at least there are no or few effects from the equilibrium between the radiation pressure and the gas pressure on radial structures of BLRs. Therefore, broad lines with accretion disk origins (Eracleous et al. 1995, Storchi-Bergmann et al. 2003, Strateva et al. 2003, Lewis et al. 2010, Zhang 2011, 2013c) are firstly considered, because of the broad lines from gravity dominated BLRs with their radial structures having few effects of the radiation pressure. For the BLR expected by the accretion disk model, the black hole gravity also dominate the dynamics of emission line clouds in BLRs, however, no equilibrium can be commonly expected between radiation pressure and gas pressure for the BLRs in accretion disk, because of much smaller ratio of radiation pressure to gas pressure than 1 expected by standard Shakura-Sunyaev accretion disk. Then, we check whether such as BLR into accretion disk can lead to positive correlation between broad line width and broad line flux.

Before proceeding further, some basic parameters of PG1613 should be given. For PG1613, the black hole mass is about  $2.8 \times 10^8 M_\odot$  reported in Peterson et al. (2004). And moreover, the BLR size is about 40 light-days determined by the reverberation mapping technique (Kaspi et al. 2000, Peterson et al. 2004). Then, We try to fit the broad balmer lines by the accretion disk origins, however, due to the single-peaked line profile without apparent double peaks nor clear shoulders, it is hard to find the unique solution. So that, the following simple disk parameters (more detailed descriptions on disk parameters can be found in Eracleous et al. 1995) are accepted to describe the observed broad H $\alpha$ : inner boundary  $r_0 = 700R_G$ , outer boundary  $r_1 = 8000R_G$  (the extended size of the disk-like BLR about 116 light-days), eccentricity  $e = 0.3$ , inclination angle  $i = 67^\circ$ , orbital phase angle  $\phi_0 = -4^\circ$ , emissivity power slope  $q = 2$  ( $f(r) \propto r^{-q}$ ) and local broadening velocity  $\sigma_{loc} = 1200\text{km/s}$ . Because the disk parameters lead to one single peaked line profile, much simi-

lar as the observed broad H $\alpha$ , we do not show the line profile expected by the elliptical accretion disk model (Eracleous et al. 1995) any more. However, It is clear that the disk parameters lead to one clear elliptical disk-like BLR into the central accretion disk of PG1613, through the detailed BLR structures, we can try to check the correlation between broad line width and broad line flux as follows.

And moreover, some simple discussions on accretion disk size are shown as follows. Hawkins (2007, 2010) have shown that optical continuum emission regions in AGN accretion disks should be less than 10 light-days, which is smaller than the extended size (116 light-days) of BLR and much smaller than the BLR size about 40 light-days of PG1613. However, we have known that for double-peaked emitters, an ion torus or a hot corona around inner accretion disk is definitely needed for illumination on the regions which produce double-peaked emission lines (the energy budget problem for double-peaked emitters, Eracleous et al. 2003). Therefore, one extra illumination source is necessary for PG1613, if the accretion disk origin is accepted for the broad lines, otherwise the longer distance from central black hole should lead to apparent energy budget problem.

Due to the much longer relativistic precession period of the accretion disk (about 230 years for inner regions of the disk-like BLR) proposed in PG1613, effects of disk precession on line profile variability can be totally ignored. Then, it is convenient to study variability of broad line having accretion disk origin, with considerations of continuum variability. Here, we make the simplifying assumption that the continuum emission propagates freely and isotropically in the central region. And moreover, we accepted that once one hydrogen cloud captures ionization photons, broad line emissions are in coinstantaneous **linear** response to ionizing continuum emissions, due to much smaller recombination time scale and much smaller resonance photon diffusion time scale (Peterson et al. 1993), and due to the strong linear correlation between continuum luminosity and broad line luminosity (Greene & Ho 2005, Zhang 2014). Then, in order to show more clear descriptions and discussions on the following results, the BLR with extended size about 116 light-days is well evenly divided into 1600 tiny regions: the radius is evenly divided into 40 bins,  $r_0 \leq r_{*,i} (i = 0, \dots, 40) \leq r_1$ , and the orbital phase angle  $\phi$  is evenly separated into 40 bins,  $0 \leq \phi_{*,j} (j = 0 \dots 40) \leq 2 \times \pi$ . Then, the observed broad line is composed of the emissions from the 1600 tiny areas. The line emission from each tiny area can be calculated by the elliptical accretion disk model ( $H(model)$ ),

$$flux_{i=0,\dots,39,j=0,\dots,39} = \int_{r_{*,i}}^{r_{*,i+1}} \int_{\phi_j}^{\phi_{j+1}} H(model) dr d\phi \quad (5)$$

Then, going with the continuum emission propagating through the extended BLR, the broad line profiles should be varying,

$$flux(t) = \sum_{i=0}^{39} \sum_{j=0}^{39} flux_{i,j}(t) \quad (6)$$

$$flux_{i,j}(t) = flux_{i,j}(t - t_0) \times \left( \frac{C_{i,j}(t)}{C_{i,j}(t - t_0)} \right)$$

where  $C_{i,j}(t)$  and  $flux_{i,j}(t)$  represents continuum and flux

intensity for the tiny region with  $r = r_{*,i}$  and  $\phi = \phi_j$  at time  $t$ , and  $t_0$  means one free time lag.

Then, based on continuum variability of PG1613 reported in Kaspi et al (2000) and the detailed BLR structure defined by the elliptical accretion disk parameters above, it is convenient to check the broad line variability by the equation (6), based on the known  $flux_{i,j}(t)$  at  $t = 0$ . Here, we have been accepted that at starting time  $t = 0$ , the same continuum intensity is for  $C_{i,j}(t)$ , which has few effects on model expected results but leads to more convenient procedure. Moreover, one time step about 4 days ( $t_0 = 4$ ) is applied in our procedure, and the procedure is stopped, once  $t$  larger than 116 (the extended size of the BLR). Then, the correlation between width and flux of model expected broad lines (about 40 data values) is shown in Figure 4. It is clear that there is one strong positive correlation between broad line width and broad line flux through the simple procedure above. The coefficient is about 0.68 with  $P_{null} \sim 10^{-6}$ . Furthermore, we can find, if model expected line parameters are used, there should be  $\log(flux) \propto 1.22 \times \log(\sigma)$ , the some large slope value 1.22 than the value listed in Equation (4) maybe due to the not well confirmed disk parameters. It is clear that the accretion disk origin can be applied to well naturally explain the unexpected positive correlation between broad line width and broad line flux for PG1613.

Besides the accretion disk origins for broad lines which indicate one totally different BLR structures from the commonly considered BLR structures, there are some other cases for the BLR with less importance of the equilibrium between the radiation pressure and the gas pressure, such as the radial flow structures in the common BLRs. However, due to the few contributions of the radial flows to the BLR size and to the total broad line width which are dominated by the gas pressure and radiation pressure, it is hardly to find the positive correlation shown in the Figure 4 due to the radial structures. Therefore, in the letter, there are no further discussions on the subtle structures in common AGN BLRs.

Before the end of the letter, we compare the positive correlations among the double-peaked emitter 3C390.3, the normal QSO PG 0052+251 and PG 1613+658. Under the mathematical formula  $\log(flux) \propto \alpha \times \log(\sigma)$ , the slope values are  $\alpha \sim 0.47 \pm 0.08$ ,  $\alpha \sim 1.83 \pm 0.12$  and  $\alpha \sim 0.96 \pm 0.08$  for the double-peaked broad H $\alpha$  of 3C390.3, for the intermediate broad optical balmer lines of PG0052+251 and for the broad optical balmer lines of PG1613+658 respectively. The different slopes probably indicate some different disk-like BLR physical parameters, which will be studied in detail in one following being prepared manuscript.

Although the detailed BLR structures are still unclear for AGN, some basic properties of BLRs can be applied to anticipate the observed broad line properties. Under the commonly accepted virialization assumption and the basic radial BLR structures for the vast majority of broad line AGNs, the strong negative correlation can be expected between broad line width and broad line flux. However, as one well theoretical model defined disk-like BLR for the broad lines with accretion disk origins, the totally gravity dominated BLR can do naturally lead to the strong positive correlation between broad line width and broad line flux. In other words, the strong positive correlation for the broad line can be used as one probable indicator for the AGN broad lines with accretion disk origins.

## ACKNOWLEDGEMENTS

Zhang, X.-G. very gratefully acknowledge the anonymous referee for giving us constructive comments and suggestions to greatly improve our paper. ZXC gratefully acknowledges the support from NSFC-11003043 and NSFC-11178003, and gratefully thanks Dr. Kaspi S. to provide public observed spectra of PG1613+658. (<http://wise-obs.tau.ac.il/~shai/PG/>).

## REFERENCES

- Baskin A., Laor A., Stern J., 2014, MNRAS, 438, 604
- Bentz, M. C., Horne, K., Barth, A., Bennert V. N., Canalizo G., et al., 2010, ApJ, 720, L46
- Bentz M. C., Denney K. D., Grier C. J., Barth A. J., Peterson B. M., et al., 2013, ApJ, 767, 149
- Blandford, R. D., & McKee, C. F., 1982, ApJ, 255, 419
- Eracleous M., Livio M., Halpern J. P., Storch-Bergmann T., 1995, ApJ, 438, 610
- Eracleous M. & Halpern J. P., 2003, ApJ, 599, 886
- Fromerth M. J. & Melia F., 2000, ApJ, 533, 172
- Greene J. E. & Ho L. C., 2005, ApJ, 630, 122
- Grier C. J., Peterson, B. M., Horne, K., Bentz, M. C., Pogge, R. W., et al., 2013, ApJ, 764, 47
- Hawkins, M. R. S., A&A, 2007, 462, 581
- Hawkins, M. R. S., MNRAS, 2010, 405, 1940
- Ho L. C., Kim M.-J., 2014, ApJ, 789, 17
- Kaspi S., Smith P. S., Netzer H., Maoz D., Jannuzi B. T., Givon U., 2000, ApJ, 533, 631
- Kaspi S., Maoz D., Netzer H., Peterson B. M., Vestergaard M., Jannuzi B. T., 2005, ApJ, 629, 61
- Kelly B. C. & Bechtold J., 2007, ApJS, 168, 1
- Kollatschny, W. & Zetzl, M. 2011, Nature, 470, 366
- Kollatschny, W. & Zetzl, M. 2013, A&A, 549, 100
- Kollatschny, W., Ulbrich, K., Zetzl, M., Kaspi, S., Haas, M., 2014, A&A, 566, 106
- Kovacevic J., Popovic L. C., Dimitrijevic M. S., 2010, ApJS, 189, 15
- Krause M., Burkert A., Schartmann M., 2011, MNRAS, 411, 550
- Lewis K. T., Eracleous M., Storch-Bergmann T., 2010, ApJS, 187, 416
- Pancoast A., Brewer B. J., Treu T., 2011, ApJ, 730, 139
- Pancoast A., Brewer B. J., Treu T., Park D., Barth A. J., Bentz M. C., Woo J.-H., 2013, submitted to MNRAS, arXiv:1311.6475
- Peterson, B. M., 1993, PASP, 105, 247
- Peterson B. M., Ferrarese L., Gilbert K. M., Kaspi, S., Malkan M. A., et al., 2004, ApJ, 613, 682
- Storch-Bergmann T., Nemmen da S. V., Strauss M. A., Hao L., Schlegel D. J., Hall P. B., et al., 2003, AJ, 126, 172
- Strateva I. V., Strauss M. A., Hao L., Schlegel D. J., Hall P. B., et al., 2003, AJ, 126, 1720
- Wang T. G., & Zhang X. G., 2003, MNRAS, 340, 793
- Woo, J.-H., Schulze A., Park D., Kang W. R., Kim S. C., Riechers D., 2013, ApJ accepted, arXiv:1305.2946
- Zhang X. G., 2011, MNRAS, 416, 2857
- Zhang X. G., 2013a, MNRAS, 429, 2274
- Zhang X. G., 2013b, MNRAS, 434, 2664
- Zhang X. G., 2013c, MNRAS Letter, 431, L112
- Zhang X. G., 2014, MNRAS, 438, 557